J|A|C|S
ARTICLES
Published on Web 02/03/2006

Charge-Localized Naphthalene-Bridged Bis-hydrazine Radical Cations

Stephen F. Nelsen,*,† Asgeir E. Konradsson,† and Yoshio Teki‡

Contribution from the Department of Chemistry, University of Wisconsin, 1101 University Avenue, Madison, Wisconsin 53706-1396, and Department of Materials Science, Osaka City University, 3-3-139 Sugimoto, Suiiyoshi-ku, Osaka 558, Japan

Received July 12, 2005; E-mail: nelsen@chem.wisc.edu

Abstract: Electron transfer (ET) in four symmetrically substituted naphthalene-bridged bis-hydrazine radical cations (1,4; 1,5; 2,6; and 2,7) is compared within the Marcus−Hush framework. The ET rate constants (k_{ET}) for three of the compounds were measured by ESR; the 2,7-substituted compound has an intramolecular ET that is too slow to measure by this method. The k_{ET} values are significantly dependent upon the substitution pattern of the hydrazine units on the naphthalene bridge but do not correlate with the distance between them. This is contrary to an assumption that is frequently made about intervalence compounds that the bridge serves only as a spacer that fixes the distance between the charge-bearing units. The internal vibrational and solvent portions (λ_v and λ_s) of the total reorganization energy (λ) have been separated using solvent effects on the intervalence band maximum, resulting in a λ_v that is the same, 9900 cm^{-1}, for the differently substituted naphthalenes. This is in accord with the general assumption that λ_v is primarily dependent upon the charge bearing unit and not the bridge. However, the trends in λ_s cannot be explained by dielectric continuum theory.

Introduction

Symmetrical, localized intervalence (IV) compounds (Robin-Day Class II)[1] that may be symbolized as **M**−**B**−**M**$^+$ provide the simplest electron transfer (ET) systems to interpret. They have an accurately known driving force for an ET ($\Delta G°$) of zero, the distance between their charge-bearing units (**M**) is controlled by the bridge (**B**), and they exhibit an IV charge-transfer band in their optical spectra. In the remarkably simple Marcus−Hush two-state classical analysis of the IV charge-transfer band,[2,3] the transition energy at the band maximum (E_{op}) is the separation between the ground- and excited-state energy surfaces at the ground-state energy minimum. This is the energy for transferring an electron without either solvent or internal geometry relaxation and equals Marcus's λ.[4,5] The electronic coupling between the **M** units at the ground-state geometry, H_{ab}, is given by eq 1, where μ_{12} is

$$H_{ab} = (|\mu_{12}|/4.8032 d_{ab})E_{op} \quad (1)$$

the transition dipole moment of the IV band (in Debye) corresponding to **M**-to-**M** charge transfer within the IV compound and d_{ab} is the distance (in Å) that the electron is transferred on the diabatic surfaces. The quantity $4.8032 d_{ab}$ corresponds to the change in dipole moment that accompanies ET, $\Delta\mu_{ab}$. Although the intervalence concept was devised for transition-metal-centered **M** units, it can also be applied to completely organic compounds.[6] We have used bicyclic hydrazines as the charge-bearing units for IV radical cations, including the 4-σ-bond-bridged **1**$^+$ and **2**$^+$ [7,8] and 5 and 9-π-bond bridged **3**$^+$ to **6**$^+$,[9−13] all of which have ET rates that are measurable by dynamic ESR except **3**$^+$, which has too large a rate constant for intramolecular ET (k_{ET}) to be accurately measured in pure solvents. These studies demonstrated that the electronic couplings (H_{ab}) between the hydrazine units determined from their

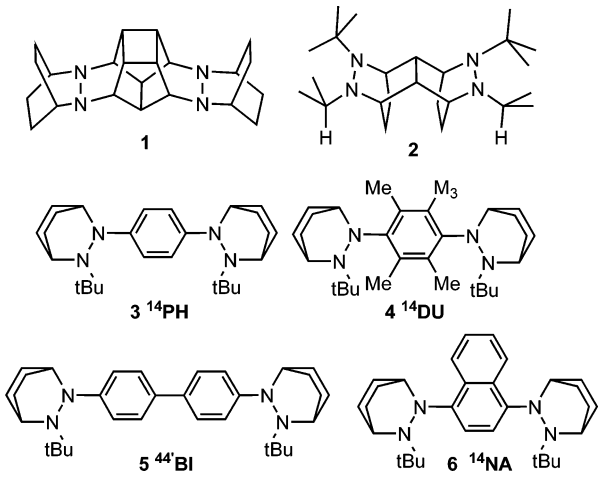

† University of Wisconsin.
‡ Osaka City University.

(1) Robin, M.; Day, P. *Adv. Inorg. Radiochem.* **1967**, *10*, 247−422.
(2) Hush, N. S. *Prog. Inorg. Chem.* **1967**, *8*, 391−444.
(3) Hush, N. S. *Coord. Chem. Rev.* **1985**, *64*, 135−457.
(4) Sutin, N. *Prog. Inorg. Chem.* **1983**, *30*, 441−499.
(5) Marcus, R. A.; Sutin, N. *Biochim. Biophys. Acta* **1985**, *811*, 265−322.

(6) We believe that Cowan and co-workers first used the term intervalence compound for an organic compound in reference to the Class III compound tetrathiofulvalene radical cation: Cowan, D. O.; LeVanda, C.; Park, J.; Kaufman, F. *Acc. Chem. Res.* **1973**, *6*, 1−7.

10.1021/ja054639k CCC: $33.50

optical absorption spectra predict k_{ET} using classical Marcus−Hush theory that employs a single reorganization energy (λ) as accurately as the electron-transfer distance (d_{ab}) that is necessary to obtain H_{ab} can be estimated. The free energy barrier obtained using the classical two-state model is given by eq 2,[2] and H_{ab}/λ is large enough for these essentially adiabatic ET reactions that all

$$\Delta G^* = \lambda/4 - H_{ab} + (H_{ab})^2/\lambda \qquad (2)$$

three terms are needed. These compounds have unusually large internal reorganization energies (λ_v) because of the large geometry change between their neutral and cationic hydrazine units, which causes problems for more modern electron transfer theory that treats λ_v effects quantum mechanically. Dynamics calculations[14] and resonance Raman measurements[15,16] indicate that the single averaged internal vibrational mode ($h\nu_v$) that ought to be employed for an intervalence hydrazine is about 800 cm^{-1}, which would make the Huang−Rhys factor $S = \lambda_v/h\nu_v$ about 12 for $\mathbf{3}^+-\mathbf{6}^+$. The size of S and the accurate separation of the high and low frequency contributions to the reorganization energy (usually called λ_v and λ_s) are crucial in applying modern ET theory[17,18] (often referred to as the Golden Rule equation).[19,20] It would require that the energy surfaces be harmonic to this vibrational level using a single mode analysis. Instead, many vibrational modes are involved for these compounds, and although a multimode analysis could in principle be done, in practice the mathematics would be extremely complex and implementing such an analysis does not seem productive, because the far simpler classical Marcus−Hush approach works quite well for calculating k_{ET} for these IV dihydrazine radical cations. Although the two-state model assumes that the electronic coupling H_{ab} is constant at all points on the electron-transfer coordinate, calculations show that this is clearly not the case for these compounds. It is well-known that H_{ab} is roughly proportional to the overlap between the charge bearing units and the bridge, which is proportional to the cosine of the twist angle between the nitrogen lone pair orbital axis and the p orbital at the carbon to which the nitrogen is attached (ϕ_{CN}) at each **M**−**B** unit. Both semiempirical AM1[21] and larger basis set ab intio UHF calculations[22] show that ϕ_{CN} is significantly smaller for the charge-delocalized transition state for ET than for either the ^{0}**M**−**B** or the more twisted $^+$**M**−**B** for the charge-localized ground state, for which the calculations successfully predict a larger $\phi_{CN(+)}$ than $\phi_{CN(0)}$ twist angle. The Hush H_{ab} eq 1 estimates the electronic coupling at the ground state, where it is far smaller than it would be at the transition state. This smaller coupling is clearly the correct one to use with eq 2 to calculate the observed rate constant. Thus, although the classical two-state equation incorrectly assumes that H_{ab} is constant as well as that ET reactions proceed through transition states instead of by the tunneling demanded by modern ET theory, the Hush evaluation of H_{ab} at the ground-state geometry from which the tunneling occurs neatly finesses this problem. It results in a significantly more accurate estimate of the rate constant for ET using classical theory than that obtained by using the far more complex Golden Rule equation with a single averaged $h\nu_v$ for these high reorganization energy compounds, because of their large S values.[9,10,12]

In this work we compare three additional naphthalene-bridged bis-hydrazine intervalence compounds $\mathbf{7}^+-\mathbf{9}^+$ with the ^{14}**NA**-bridged compound $\mathbf{6}^+$. Compounds **3**−**10** have the same **M** groups, the 2-*tert*-butyl-2,3-diazabicyclo[2.2.2]oct-3-yl that we will abbreviate as **Hy**. Despite the bridge being the same for $\mathbf{6}^+-\mathbf{9}^+$, their electron-transfer rate constants and optical spectra vary significantly and show no correlation with the distance between their **Hy** group, despite the dominance this parameter has had in discussions of ET through bridges.[3]

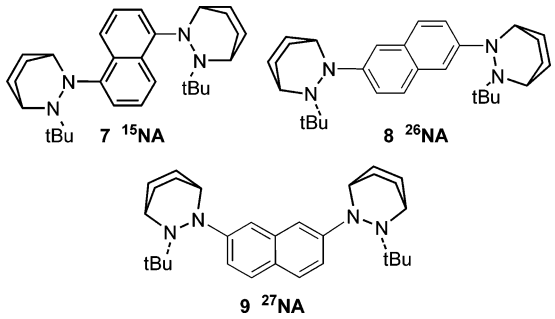

Results

ESR Measurement of ET Rate Constants. Monohydrazines **10** and **11** were also studied as models for the bis-hydrazines. The neutral compounds were prepared, as in our previous work, by reaction of mono- or dilithionaphthalene with the diazenium salt 2-*tert*-butyl-2,3-diazabicyclo[2.2.2]octene iodide.[23] Since these are localized IV compounds, their redox potentials are principally determined by the **Hy** unit. The first oxidation potentials for these compounds are in the range 0.10−0.22 V versus the saturated calomel electrode in acetonitrile and second oxidation potentials for the disubstituted compounds in the range 0.34−0.38 V. The $E^\circ_2 - E^\circ_1$ values fall in the order 0.27 V

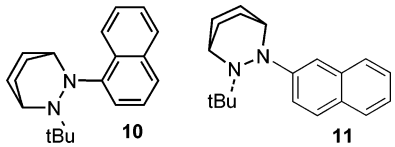

(7) Nelsen, S. F.; Chang, H.; Wolff, J. J.; Adamus, J. *J. Am. Chem. Soc.* **1993**, *115*, 12276−12289.
(8) Nelsen, S. F.; Adamus, J.; Wolff, J. J. *J. Am. Chem. Soc.* **1994**, *116*, 1589−1590.
(9) Nelsen, S. F.; Ismagilov, R. F.; Trieber, D. A., II. *Science* **1997**, *278*, 846−849.
(10) Nelsen, S. F.; Ismagilov, R. F.; Powell, D. R. *J. Am. Chem. Soc.* **1996**, *118*, 6313−6314.
(11) Nelsen, S. F.; Ismagilov, R. F.; Powell, D. R. *J. Am. Chem. Soc.* **1997**, *119*, 10213−10222.
(12) Nelsen, S. F.; Ismagilov, R. F.; Gentile, K. E.; Powell, D. R. *J. Am. Chem. Soc.* **1999**, *121*, 7108−7114.
(13) Nelsen, S. F.; Ismagilov, R. F. *J. Phys. Chem. A* **1999**, *103*, 5373−5378.
(14) Nelsen, S. F. *J. Am. Chem. Soc.* **1996**, *116*, 2047−2058.
(15) Williams, R. D.; Hupp, J. T.; Ramm, M. T.; Nelsen, S. F. *J. Phys. Chem. A* **1999**, *103* 11172−11180.
(16) In resonance Raman work done in collaboration with J. V. Lockard and J. E. Zink, to be published separately, for $\mathbf{6}^+$ (^{14}**DU**$^+$), the relative intensities for 13 observed resonance-enhanced bands produce $h\nu_v$ = 796 cm^{-1}.
(17) Ulstrup, J.; Jortner, J. *J. Chem. Phys.* **1975**, *63*, 4358−4368.
(18) Bixon, M.; Jortner, J. *Adv. Chem. Phys.* **1999**, *106*, 35−202.
(19) Closs, G. L.; Calcaterra, L. T.; Green, N. J.; Penfield, K. W.; Miller, J. R. *J. Phys. Chem.* **1986**, *90*, 3673−3683
(20) Closs, G. L.; Miller, J. R. *Science* **1988**, *240*, 440−448.
(21) Nelsen, S. F.; Blomgren, F. *J. Org. Chem.* **2001**, *66*, 6551−6559.
(22) Blomgren, F.; Larsson, S.; Nelsen, S. F. *J. Comput. Chem.* **2001**, *22*, 655−664.
(23) Nelsen, S. F.; Konradsson, A. E.; Weaver, M. N.; Guzei, I.; Göbel, M.; Wortmann, R.; Lockard, J. V.; Zink, J. I. *J. Phys. Chem. A.* **2005**, *109*, 10854−10861.

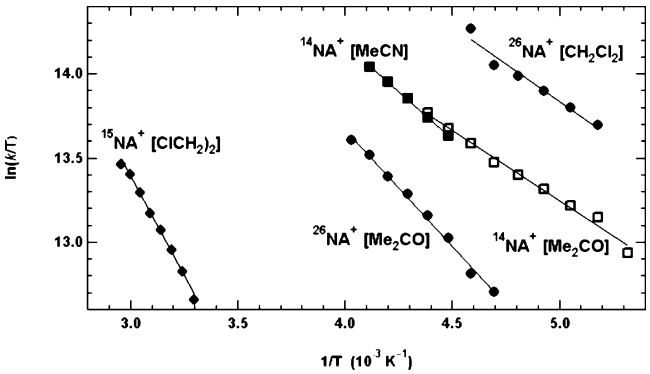

Figure 1. Eyring plots of ESR kinetic data for naphthalene-bridged bis-hydrazine radical cations.

(**^{14}NA**), 0.20 V (**^{26}NA**), and 0.16 V (**^{15}NA** and **^{27}NA**). Details appear in the Supporting Information.

The cations were prepared by oxidation with silver salts. The rate constants for intramolecular exchange within the bis-hydrazine radical cations were determined by simulating their ESR spectra. In the small k_{ET} limit the unpaired electron is localized on one hydrazine unit on the ESR time scale, producing a 1:2:3:2:1 pattern for coupling to two equivalent nitrogens. Although the nitrogens of each hydrazine are not quite the same, their hyperfine splitting constants are too close to resolve by ESR. In the large k_{ET} limit a nine-line pattern for coupling to all four nitrogens is observed, and when k_{ET} is near 10^8 s^{-1}, an alternating line width effect is seen and a very accurate measurement of k_{ET} results. **8**$^+$ **^{26}NA** showed only the nine-line pattern down to the temperature where acetonitrile (AN) froze, so it was too fast to measure by ESR in this solvent. Its ET kinetics were determined in the lower melting and lower λ_s solvents methylene chloride (MC) and acetone. The temperatures available are all above the temperature of maximum broadening so the rate constant data are not as accurate as they would have been if lower temperatures could also have been investigated. ET rate constants for bis-hydrazines are significantly larger (on the order of a factor of 5) in MC than they are in AN. Nevertheless, ion pairing in MC makes them slower than they would be for the free ion, as has been demonstrated for **4**$^+$, **5**$^+$, and other examples.[13] **6**$^+$ **^{14}NA** was also studied here in acetone; its kinetics in acetonitrile were reported previously.[12] **7**$^+$ **^{15}NA** showed such slow ET that it could only be studied at relatively high temperatures in low λ_s solvents, so it was studied in 1,2-dichloroethane (which is similar in its properties to methylene chloride but less volatile). **9**$^+$ **^{27}NA** showed only the five-line pattern in all solvents, so its intramolecular ET is too slow to measure by ESR. The rate constants determined by spectral simulation are listed in the Supporting Information and shown as Eyring plots in Figure 1, and the activation parameters are listed in Table 1. The ranges quoted in Table 1 include statistical error only. The enthalpies

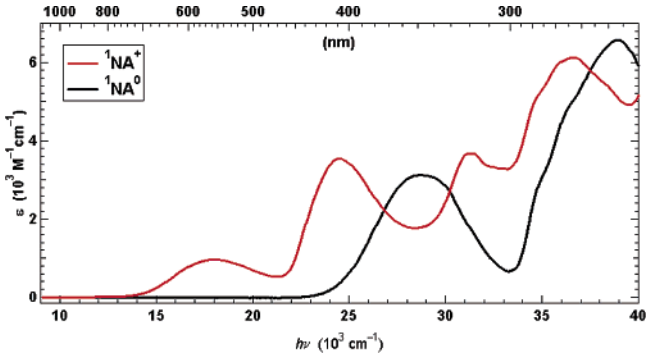

Figure 2. Absorption spectra for neutral and cationic **10** (**^{1}NA**) in acetonitrile.

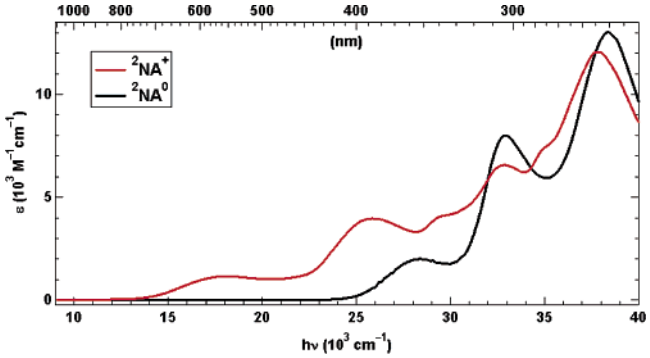

Figure 3. Absorption spectra for neutral and cationic **11** (**^{2}NA**) in acetonitrile.

of activation are much more certain than the entropies, so we compare the rate constants at 215 K, which is within the temperature range studied for four of the five data sets available for naphthalene-bridged hydrazine-centered systems. The k_{ESR} values are quite close for **^{14}NA**$^+$ and **^{26}NA**$^+$, but **^{14}NA**$^+$ has a 2.2 times larger rate constant in acetone at 215 K. **^{26}NA**$^+$ has about a 100-fold larger k_{ET} value than the **^{15}NA**$^+$ in comparable solvents, methylene chloride and dichloroethane, respectively.

Solvent Effects on Optical Absorption Spectra and λ_s Determination. The absorption spectra of the neutral and radical cation oxidation levels of the monohydrazines are compared in Figures 2 and 3. **10**$^+$ (**^{1}NA**$^+$) shows two bands at lower energy than the lowest energy band for the neutral compound, at ~18 000 cm^{-1} (555 nm) and 24 500 cm^{-1} (408 nm), while **11**$^+$ (**^{2}NA**$^+$) has bands at ~18 000 cm^{-1} and 25 700 cm^{-1} (389 nm). We assign the visible bands to charge transfer from the aryl ring to the hydrazine radical cation group, which is largely localized at the NN$^+$ 3e-π bond, and will refer to such bands as aryl oxidation (AO) bands.

The bis-α and bis-β-substituted radical cations are compared with their monohydrazine analogues in Figures 4 and 5. Three of the four bis-hydrazines show a Hush-type superexchange band (which we will refer to as SE bands and their band

Table 1. Eyring Activation Parameters from the ESR Data for Naphthalene-Bridged Bis-hydrazines

	7$^+$$NO_3^-$ **^{15}NA** in $(ClCH_2)_2$	**8**$^+$$NO_3^-$ **^{26}NA** in CH_2Cl_2	**8**$^+$$NO_3^-$ **^{26}NA** in Me_2CO	**6**$^+$$SbF_6^-$ **^{14}NA** in Me_2CO	**6**$^+$$SbF_6^-$ **^{14}NA** in MeCN[a]
R^2	0.997	0.978	0.997	0.994	0.999
$\Delta H^{\ddagger}$[b]	4.7 ± 0.3	1.8 ± 0.4	2.8 ± 0.2	1.7 ± 0.14	2.7 ± 0.7
$\Delta S^{\ddagger}$[c]	−6.6 ± 0.9	−10.9 ± 2.1	−9.0 ± 0.8	−12.6 ± 0.7	−8.0 ± 3.0
k_{ESR}(215 K)	2.7×10^6	2.8×10^8	6.9×10^7	1.5×10^8	1.4×10^8

[a] Data from ref 12. [b] Unit: kcal/mol. [c] Unit: cal/mol deg.

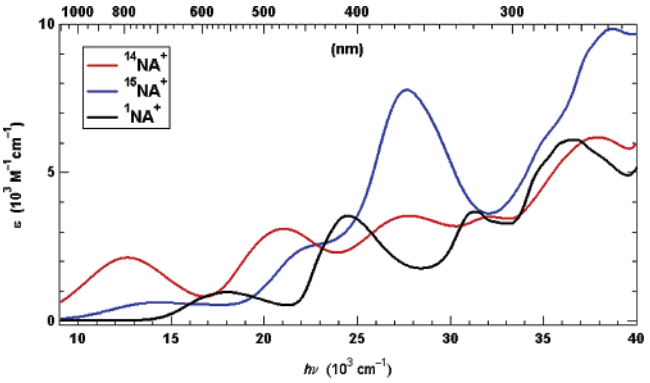

Figure 4. Optical absorption spectra for the α-substituted naphthalene radical cations $\mathbf{10}^+$ ($^{1}\mathbf{NA}^+$), $\mathbf{6}^+$ ($^{14}\mathbf{NA}^+$), and $\mathbf{7}^+$ ($^{15}\mathbf{NA}^+$).

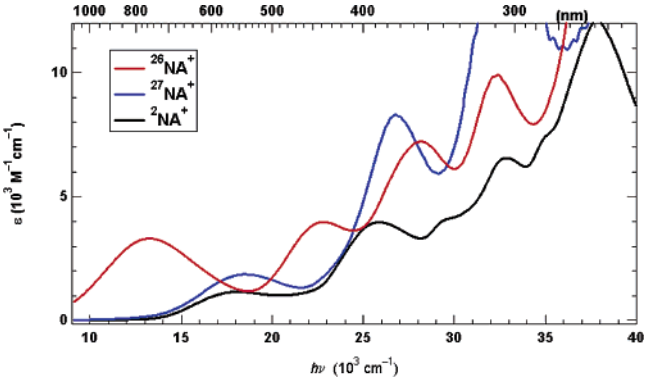

Figure 5. Optical absorption spectra for the β-substituted naphthalene radical cations $\mathbf{11}^+$ ($^{2}\mathbf{NA}^+$), $\mathbf{8}^+$ ($^{26}\mathbf{NA}^+$), and $\mathbf{9}^+$ ($^{27}\mathbf{NA}^+$).

maxima, which correspond to λ values in Marcus−Hush theory, as E_{op}) at distinctly lower energy than that of the AO band of the monohydrazines. $^{26}\mathbf{NA}^+$ and $^{14}\mathbf{NA}^+$ clearly have larger SE bands than $^{15}\mathbf{NA}^+$, as expected from their larger k_{ESR} values. The non-Kekulé substitution pattern compound, $^{27}\mathbf{NA}^+$, does not show a detectable SE band, which is consistent with the much slower ET indicated by its ESR.

Ion pairing occurs for bis-hydrazine radical cations in methylene chloride, as has been established by concentration studies of the SE band maximum for three aromatic bridged compounds, including $\mathbf{4}^+$ and $\mathbf{6}^+$,[13] and two saturated-bridged ones.[24] The results of fits of dilution studies similar to those of the previous work are shown in Figures 6 and 7 and establish the free ion and ion paired E_{op} values shown in Table 2. The ion pairing equilibrium constants K_{IP} obtained have large standard errors (±4350 M^{-1} for $\mathbf{7}^+\mathbf{NO_3}^-$ and ±204 M^{-1} for $\mathbf{8}^+\mathbf{NO_3}^-$), but the ion pairing free energy values, $\Delta G°_{IP} = -RT \ln K_{IP}$, are notably insensitive to structure, as shown by the value obtained for tetrabutylammonium chloride (last column, Table 2), which is comparable to the values for the seven bis-hydrazine radical cations studied (total range −4.5 to −5.3 kcal mol^{-1}).[13,24] There is little correlation of these values with structure, and we suggested that the principal determinate of K_{IP} is how different the distances are between the counterion and the neutral and cationic charge-bearing hydrazine units. This view was borne out by study of crystalline $\mathbf{3}^+$ and $\mathbf{4}^+$, where the distances have been determined crystallographically.[25] The only crystal structure available in this series is one for $\mathbf{7}^{2+}(\mathbf{BPh_4}^-)_2$,[26] which has the counterions positioned away from the bridge, instead of over the bridge as it is for $\mathbf{3}^+\mathbf{BPh_4}^-$, $\mathbf{4}^+\mathbf{BPh_4}^-$, and the 2,5-dimethyl-1,4-phenylene-bridged bis(BPh_4^-) salt.[10] Although a range of counterion placements is obviously sampled in solution, a preponderance of the placement shown, which may be the most stable for the cation as well as the dication, would be consistent with the K_{IP} value found, which is the largest of the seven compounds studied.

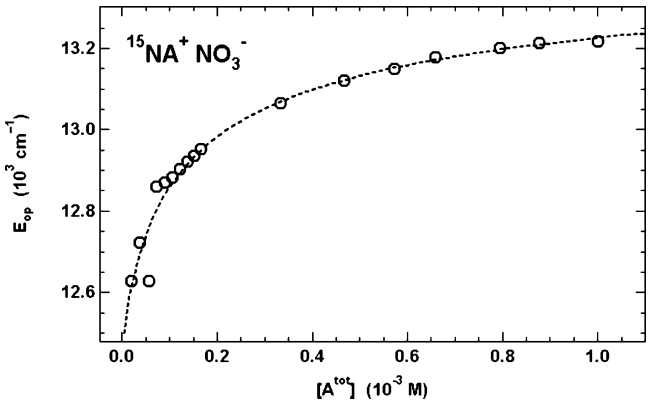

Figure 6. Ion pairing studies for methylene chloride solutions of $\mathbf{7}^+$ ($\mathbf{NO_3}^-$). Dashed lines are fits to the ion pairing equilibrium.[13,24]

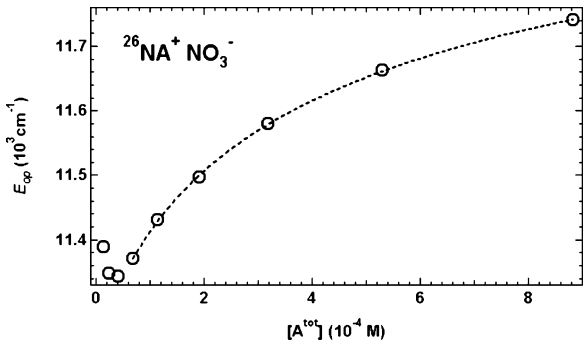

Figure 7. Ion pairing studies for methylene chloride solutions of $\mathbf{8}^+$ ($\mathbf{NO_3}^-$). Dashed lines are fits to the ion pairing equilibrium.[13,24]

Table 2. Ion Pairing Parameters for NA-Bridged Bis-hydrazine Radical Cation Nitrates and Tetrabutylammonium Chloride in Methylene Chloride

compound	$\mathbf{7}^+NO_3^-$	$\mathbf{8}^+NO_3^-$	$\mathbf{Bu_4N}^+$
bridge	$^{15}\mathbf{NA}^+$	$^{26}\mathbf{NA}^+$	
K_{IP}, M^{-1}	ca. 9700	ca. 3200	ca. 6300
$\Delta G°_{IP}$, kcal mol^{-1}	−5.3	−4.7	−5.1
E_{op}^{free}, cm^{-1}	12 460	11 269	
E_{op}^{IP}, cm^{-1}	13 510	12 190	
$\Delta G°_{IP,ET}$, kcal mol^{-1}	3.0	2.7	

Ion pairing is exoenergetic, so more ion pairs are present at higher concentration, and the values observed are consistent with significant amounts of ion pairing at the approximately millimolar concentrations of the ESR measurements. Ion pairing raises the reorganization energy for ET, because the electron transfer produces material with the ion next to the neutral hydrazine unit. We estimate the free energy difference as $\Delta G°_{ET,IP} = E_{op}^{IP} - E_{op}^{free}$ and also include these numbers in Table 2. Although detectable, the increase in λ has a relatively small effect on k_{ESR}.[13]

(24) Nelsen, S. F.; Trieber, D. A., II; Ismagilov, R. F.; Teki, Y. *J. Am. Chem. Soc.* **2001**, *123*, 5684−5694.
(25) Nelsen, S. F.; Konradsson, A. E.; Clennan, E. L.; Singleton, J. *Org. Lett.* **2004**, *6*, 285−287.
(26) Nelsen, S. F.; Konradsson, A. E.; Ismagilov, R. F.; Guzei, I. A. *Cryst. Growth Des.* **2005**, *5*, 2344−2347.

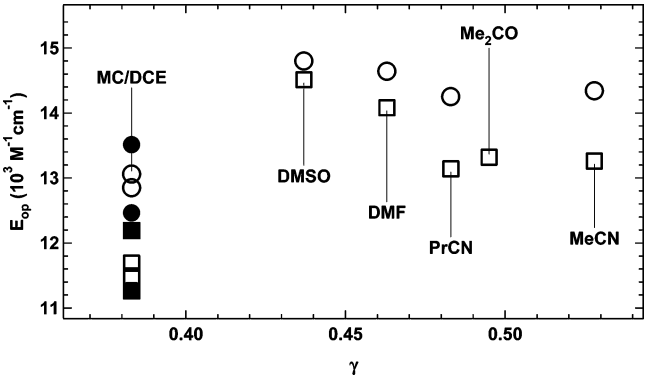

Figure 8. Plots of E_{op} versus γ for $\mathbf{7}^+$ ($^{15}\mathbf{NA}^+$), circles, and $\mathbf{8}^+$ ($^{26}\mathbf{NA}^+$), squares. The E_{op}^{free} and E_{op}^{IP} values for the nonpolar solvents (the only one in this series expected to show detectable ion pairing) are shown as filled symbols.

Table 3. E_{Op}, γ, and DN Values for the Solvents Used

solvent	γ	DN	$E_{op}(\mathbf{7}^+)$	$E_{op}(\mathbf{8}^+)$
acetonitrile (MeCN)	0.528	14.1	14 340	13 260
acetone (Me_2CO)	0.495	17.0		13 320
butyronitrile (PrCN)	0.483	16.6	14 250	13 140
DMF ($Me_2NC(=O)H$)	0.463	26.6	14 640	14 080
DMSO (Me_2SO)	0.437	29.8	14 800	14 510
DCE ($(ClCH_2)_2$)	0.382	0.0	13 060	11 690
MC (CH_2Cl_2)	0.383	0.0	12 850	11 490
E_{op}^{free} in MC			12 460	11 260
E_{op}^{IP} in MC			13 510	12 190

We shall next consider separating the vibrational and solvent components, λ_v and λ_s, of the total reorganization energy, $\lambda = E_{op}$. We recently discussed this in detail for previously studied dinitrogen-centered radical cations.[24] Although dielectric continuum theory assumes that λ will be proportional to the solvent parameter $\gamma = 1/\epsilon_S - 1/n^2$, this is clearly not the case for dinitrogen-centered radical cations, including those studied here; see Figure 8. As discussed previously, a better correlation for the solvents we have studied is actually seen plotting E_{op} versus Gutmann donor number (DN, see Table 3),[27] and a linear correlation is seen using eq 3, which includes different slopes for additive terms correlating the data with γ and DN (see Figures 9 and 10).

$$E_{op}[\text{calcd}] = A + B\gamma + D\text{DN} \qquad (3)$$

It should be noted that because DN = 0 for methylene chloride, the E_{op} and E_{op}[calcd] points lie on top of each other for this solvent. The relative sizes of the solvent donicity increments are given by the vertical deviations in these plots. The fitting parameters obtained are compared with those for other aromatic bis-hydrazines in Table 4. We equate *A*, the solvent independent portion, with λ_v, which makes λ_v 9900 cm^{-1} for the **NA**-bridged compounds. To a first approximation, λ_v should only depend on the charge-bearing unit, and the average value is 9850 cm^{-1}, with a total range of 600 cm^{-1} (6% of the smallest value), which is consistent with the separation of λ_s and λ_v by the above method being successful. Equating λ_s in each solvent with $E_{op} - \lambda_v$ gives the data in Table 5, which are presented in order of increasing closest N,N distance. Although dielectric continuum theory assumes that the only factor caused by the bridge that affects λ_s is the distance between the charge-bearing units, our data clearly show that this is not the case. Not only is the solvent donicity important (it has nothing to do with dielectric continuum theory) but also saturated bridges produce substantially larger λ_s values for a given distance than do the aromatic ones studied here.[24] For both aromatic and saturated bridges, there is indeed a trend to higher λ_s as the N,N distance increases, but methylation of the ring without changing the distance (^{14}**DU** versus ^{14}**PH** bridges) increases λ_s (by 20−70%, depending upon solvent) and decreasing the distance with a

(27) Gutmann, V. *The Donor−Acceptor Approach to Molecular Interactions*; Plenum: New York, 1980.

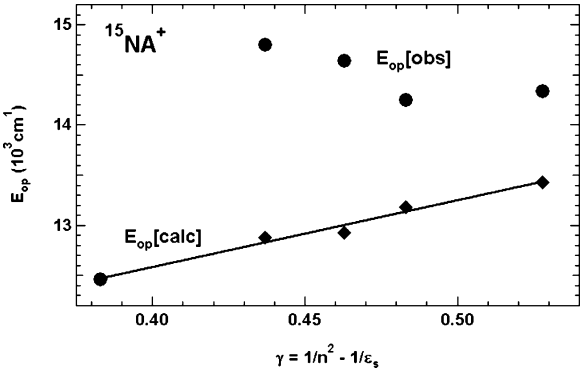

Figure 9. E_{op} (circles) and E_{op}[calcd] (diamonds) versus γ plots for $\mathbf{7}^+\mathbf{NO_3}^-$ $^{15}\mathbf{NA}^+$.

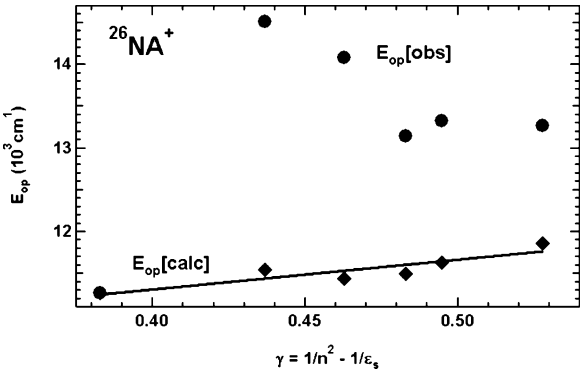

Figure 10. E_{op} (circles) and E_{op}[calcd] (diamonds) versus γ plots for $\mathbf{8}^+\mathbf{NO_3}^-$ $^{26}\mathbf{NA}^+$.

Table 4. Fitting Parameters (in cm^{-1}) for Aromatic Bridged Bis-hydrazine Radical Cations

compd	bridge	$A = \lambda_v$	*B*	*D*	RMS[b]
$\mathbf{7}^+$	^{15}**NA**	9920	6662	65	46
$\mathbf{8}^+$	^{26}**NA**	9900	3521	100	85
$\mathbf{3}^+$	^{14}**PH**[a]	9810	5600	32	21
$\mathbf{4}^+$	^{14}**DU**[a]	10 100	5800	69	65
$\mathbf{5}^+$	$^{44'}$**BI**[a]	9500	9100	70	55

[a] From ref 24. [b] The RMS (error) is $[\Sigma(\text{Dev})^2/n]^{1/2}$, where "Dev" is E_{op}[calcd] (eq 3) − (regression line value) and *n* is the number of solvents used.

Table 5. λ_s Values (cm^{-1}) for Five Aromatic-Bridged Bis-hydrazines

bridge	*d*(N,N)	λ_s (AN)	λ_s (PrCN)	λ_s (DMF)	λ_s (DMSO)	λ_s (Me_2CO)	λ_s (MC)
^{14}**PH**[a]	5.7	3400		3400		3300	1300
^{14}**DU**[a]	5.7	4000	3900	4600	4500	4200	2200
^{15}**NA**	6.16	4400	4300	4700	4900		2500
^{26}**NA**	7.86	3400	3200	4200	4600	3400	1400
$^{44'}$**BI**[a]	10.0	5700	5600	6000	6100	5800	3500

[a] Previously unpublished numbers from the Ph.D. thesis of Dwight A. Trieber II, University of Wisconsin, Madison, 2000.

naphthalene bridge in going from **^{26}NA** to **^{15}NA** increases λ_s by (by 10 to 80%, depending upon solvent) instead of decreasing it.

Prediction of ET Rate Constants from the Optical Spectra. The optical spectra were studied between about 255 and 325 K to allow calculation of the optically determined rate constants. As discussed in detail previously for other aromatic and saturated-bridged hydrazines,[9,10,12] classical Marcus−Hush theory works considerably better for predicting rate constants from the optical spectra for these high λ compounds than does the Bixon−Jortner implementation of vibronic coupling theory, also called the Golden Rule equation.[17,18,28] Because the vibrational reorganization energy (λ_v) is about 9900 cm^{-1} for these compounds and the averaged barrier-crossing frequency ($h\nu_v$) appropriate for hydrazines is about 800 cm^{-1},[14,15] the ET surfaces for these compounds would have to remain harmonic past $S = \lambda_v/h\nu_v = 12$ for this approach to work quantitatively, and they rather clearly do not. We instead use a classical Marcus−Hush type analysis, but the IV band shape shows that the diabatic surfaces are not always perfect parabolas, because the SE bands are mostly broader than the $(16\ RT\ \ln(2)\ E_{op})^{1/2}$ value that Hush pointed out would occur for parabolic diabatic surfaces using classical theory.[2] The bands may be fit as well using only λ and a quartic fitting parameter (called Q here) by adding a quartic term to the Marcus−Hush parabolas by using the three parameters required using the Golden Rule equation (λ_v, λ_s, and $h\nu_v$). We also include the refractive index correction to ϵ_{max} that was introduced for extracting electronic couplings from optical spectra by the Kodak group,[29] which has the effect of inserting a factor of $N = 3n^{1/2}/(n^2 + 2)$ into the equation Liptay used for calculating the transition dipole moment (μ_{12}), eq 4, and also into Hush's formula for calculating the electronic

$$|\mu_{12}| = \left(\frac{1000\ \ln(10)\ 3hc}{8\pi^3 N_A}\int_{band}\frac{\epsilon(\bar{\nu})}{\bar{\nu}}\,d\bar{\nu}\right)^{1/2} = 0.09584\cdot\left(\int_{band}\frac{\epsilon(\bar{\nu})}{\bar{\nu}}\,d\bar{\nu}\right)^{1/2} \quad (4)$$

coupling H_{ab}, eq 1. Although N is a rather small correction (a factor of 0.914 in acetonitrile and 0.890 for methylene chloride at room temperature), it improves the agreement of the optical with the ESR rate constants. Liptay's eq 4 gives results very similar to those using Hush's familiar Gaussian approximation, about 1−2% higher for the compounds studied here, leading to only about a 0.25−0.35% change in the d_{ab} that is obtained; we certainly do not know d_{ab} to this accuracy.[30] We follow Hush in using $\Delta\mu_{ab} = e\ d_{ab}$ in eq 1 and use Cave and Newton's Generalized Mulliken−Hush eq 5[31]

$$d_{ab}^{\ 2} = d_{12}^{\ 2} + 4(|\mu_{12}|/e)^2 \quad (5)$$

to relate d_{12}, the electron-transfer distance on the adiabatic surface, to that on the diabatic surface, the d_{ab} that is necessary for use in eq 1. The difference between d_{ab} and d_{12} is rather small for all of these compounds. Estimating d_{12} requires consideration of the conformational complexity of these compounds.[32] α-**Hy**-substituted naphthalenes (the α positions are 1, 4, 5, and 8) are significantly more stable when the NN bond is syn to the adjacent β carbon (β positions are 2, 3, 6, and 7), so the NN bond is more stable syn to position 2 for a 1-substituted compound than syn to the bridgehead carbons, for obvious steric reasons. β-Hy-substituted naphthalenes, on the other hand, have sterically almost equivalent conformations with the NN bond syn to α and β carbons. As shown in Table 6, AM1 calculations get the conformations having the NN bond syn to the adjacent α carbon to be slightly more stable than those syn to the adjacent β carbon. For each of the NN bond rotation conformations there are energy minima with the *tert*-butyls syn and anti. The four diastereomeric conformations for **^{14}NA**$^+$ are calculated by AM1 to lie within 0.1 kcal/mol of each other, so all will contribute to the observed experiments, but their dipole moments and hence d_{12} values are calculated to lie within 0.01 Å of being the same. We calculate d_{12} from the dipole moment calculated for localized IV compounds, which we call d_μ to distinguish them from d_{12} estimated by other means, as $d_\mu(Å) = 2\mu_1(D)/4.8032$, where μ_1 is the dipole moment in the electron-transfer direction (calculated here using the in-plane components of the dipole vector).[33,33] Table 7 contains values calculated using both AM1 semiempirical and UHF/6-31G* ab initio calculations. As we have noted elsewhere, DFT calculations such as B3LYP are useless for this purpose, because although they partially localize charge, they get the geometries nearly the same for oxidized and neutral **Hy** units,

Table 6. Calculated ET Distances (Å) Derived from Dipole Moments for Hy_2NA^+ Isomers

			AM1 calculation				UHF/6-31G* calculation				
bridge	NN syn[a]	*t*Bu	$\Delta\Delta H_f$[b]	d_μ	d_{NN}	ratio	d_μ	d_{NN}	ratio	d_{ESR}	d_{opt}[c]
^{14}PH	2,3	syn		4.47	5.70	0.78	4.81	5.65	0.85		
^{14}XY[d]	3,6	anti		4.71	5.71	0.82	4.71	5.64	0.84	5.25	
^{14}DU	2,3	syn		4.58	5.70	0.80	4.71	5.65	083	5.66	
^{14}NA	2,3	syn	0	4.63	5.72	0.81	4.57	5.66	0.81		4.61
	2,3	anti	0.08	4.64	5.72	0.81					
^{15}NA	2,6	syn	0	5.43	6.22	0.87	5.39	6.16	0.88	6.49	6.49
	2,6	anti	0.07	5.43	6.22	0.87					
^{26}NA	1,5	syn	0	6.35	7.95	0.80	6.29	7.86	0.80		6.40
	3,5	anti	0.05	5.87	7.93	0.74	6.33	7.86	0.81		
	3,7	syn	0.11	6.26	7.91	0.79					
^{27}NA	1,8	syn	0	5.85	7.41	0.79					
	1,6	syn	0.28	6.06	7.42	0.82					
	3,6	syn	0.60	6.39	7.34	0.94				7.37	7.37

[a] Conformation with NN group syn to the carbon numbers shown. [b] Difference in heat of formation from that of the most stable diastereomeric conformation calculated using UHF/AM1. [c] d_{opt} is the d_{12} value that was used in calculating the H_{ab} values and rate constants in Table 7. [d] The **^{14}XY** bridge is 2,5-dimethyl-1,4-phenylene.[10]

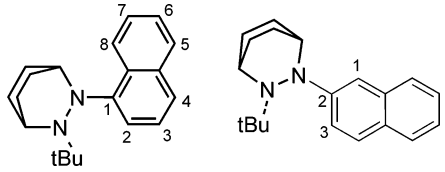

(28) Jortner, J.; Bixon, M. *J. Chem. Phys.* **1988**, *88*, 167−170.
(29) (a) Gould, I. R.; Noukakis, D.; Gomez-Jahn, L.; Young, R. H.; Goodman, J. L.; Farid, S. *Chem. Phys.* **1993**, *176*, 439−456. (b) Gould, I. R.; Young, R. H.; Albrecht, A. C.; Mueller, J. L.; Farid, S. *J. Am. Chem. Soc.* **1994**, *116*, 8188−8199.
(30) For further discussion, see the thesis of Ageir E. Konradsson, University of Wisconsin, 2004, p 84.
(31) (a) Newton, M. D.; Cave, R. J. *Molecular Electronics*; Jortner, J.; Ratner, M., Eds.; Blackwell Science: Oxford, 1997; p 73. (b) Cave, R. J.; Newton, M. D. *Chem. Phys. Lett.* **1996**, *249*, 15−19. (c) Cave, R. J.; Newton, M. D. *J. Chem. Phys.* **1997**, *106*, 9213−9226. (d) Newton, M. D. *Adv. Chem. Phys.* **1999**, *106*, Pt. 1, 303−375.
(32) Nelsen, S. F.; Newton, M. D. *J. Phys. Chem. A* **2000**, *104*, 10023−10031.
(33) Johnson, R. C.; Hupp, J. T. *J. Am. Chem. Soc.* **2001**, *123*, 2053−2057.

Table 7. Room Temperature Optical Simulation Parameters for NA-Bridged Hydrazine Radical Cations

compd	bridge	solvent	Q	E_{op}[a]	μ_{12}[b]	H_{ab}[a,c]	k_{opt}[d]
$\mathbf{6}^+$	$^{14}\mathbf{NA}^+$	MeCN	0.008	12 640	3.05	1510	32
$\mathbf{7}^+$	$^{15}\mathbf{NA}^+$	$(ClCH_2)_2$	0.070	13 060	1.71	620	0.9
$\mathbf{8}^+$	$^{26}\mathbf{NA}^+$	Me_2CO	−0.018	13 300	3.29	1300	5.2
$\mathbf{8}^+$	$^{26}\mathbf{NA}^+$	CH_2Cl_2	0.125	11 490	4.46	1410	220
$\mathbf{9}^+$	$^{27}\mathbf{NA}$	MeCN	[0]	14 180[e]	0.62	230	0.004

[a] Unit: cm^{-1}. [b] Unit: Debye. [c] Calculated using the d_{opt} values of Table 7 as d_{12}. [d] At 25 °C, Unit: 10^8 s^{-1}. [e] Maximum of the simulated SE band.

which is known from X-ray crystal structures not to be correct.[10] The UHF/6-31G* d_μ values for $^{14}\mathbf{PH}^+$, $^{14}\mathbf{XY}^+$, and $^{14}\mathbf{DU}^+$ do not show the anomaly of the middle value being the higher than the AM1 values, but it is still not obvious that they are correct. A quite different and experimental way of estimating d_{12} is to use the triplet diradical dication as a model.[11] We suggested that the average distance between the odd electrons in the dication (which we call d_{ESR}) is very similar to the concept of the average distance for electron transfer in the radical cation. The triplet dication dipolar ESR splitting constant, D' (cm^{-1}), can be converted to d_{ESR} using d_{ESR} (Å) = $1.3747(1/D'^3)$.

Unfortunately the dication diradicals are too unstable to make the measurement for $^{14}\mathbf{PH}^{2+}$, $^{14}\mathbf{NA}^{2+}$, and $^{26}\mathbf{NA}^{2+}$, but these measurements have been made in Osaka for the other compounds of Table 7. The ESR spectrum of triplet $^{15}\mathbf{NA}^{2+}(\mathbf{SbF_6}^-)_2$ was studied in a 1:1:1 CH_3CN/nPrCN/CH_2Cl_2 glass between 20 and 80 K, and simulation of the 60 K spectrum gave D = 0.0095 cm^{-1}, E = 0.0005 cm^{-1}. The ESR signal became stronger at lower temperature, indicating that the ground state is a triplet, in contrast to $^{14}\mathbf{DU}^{2+}$, which has a higher H_{ab} value, and is a ground-state singlet.[34] The temperature dependence of the magnetic susceptibility measured by SQUID was analyzed using the dimer model of $S = 1$ species, giving an intermolecular antiferromagnetic interaction of J/k = −19.8 K. The SQUID measurement indicated a 4% impurity of radical cation. The ESR spectrum of $^{27}\mathbf{NA}^{2+}(SbF_6^-)_2$ was studied in a 1:1:1 CH_3CN/nPrCN/CH_2Cl_2 glass between 10 and 80 K, and simulation of the 10 K spectrum gave D = 0.0065 cm^{-1}, E = 0.0 cm^{-1}. The ESR signal intensity increased as the temperature was lowered, showing that the triplet state is the ground state, as expected for this non-Kekulé substitution pattern compound.[35] The temperature dependence of the magnetic susceptibility measured by SQUID was well analyzed using the triplet−singlet model (triplet ground state) with J/k = 33.4 K and a weak intermolecular antiferromagnetic interaction of −0.33 K. As discussed previously,[10] better agreement between k_{ESR} and k_{opt} is obtained using the larger d_{ESR} than by using d_μ, and we therefore also use the d_{ESR} values for $\mathbf{9}^+$ and $\mathbf{10}^+$.

We used the semiclassical adiabatic rate eq 6

$$k_{opt} = \kappa_{el} 2.40 \times 10^{13} (\lambda_v/\lambda)^{1/2} \exp(-\Delta G^*/RT) \qquad (6)$$

to calculate rate constants from our optical data. The constant 2.40×10^{13} corresponds to an $h\nu_v$ of 800 cm^{-1}. $^{14}\mathbf{NA}^+$ and $^{26}\mathbf{NA}^+$ have large enough electronic transmission coefficients $(\kappa^{el})^{4,eq}$ [36] that they are indistinguishable from 1.0, and even $^{15}\mathbf{NA}^+$ has a κ_{el} of 0.9 or larger. The 9900 cm^{-1} λ_v obtained from the solvent studies was used for all three compounds, and as previously discussed,[9] ΔG^* may be calculated including the quartic correction Q using eq 7.

$$\Delta G^* = \frac{1 + Q/4}{(1 + Q)} \cdot \frac{\lambda}{4} - H_{ab} + \frac{H_{ab}^2}{\lambda} \qquad (7)$$

The optical data as a function of temperature for the solvents used for the ESR rate constant studies are tabulated in the Supporting Information,[36] and Figures 11−13 compare the data graphically. Agreement is remarkably good for the $^{14}\mathbf{NA}$- and $^{15}\mathbf{NA}$-bridged compounds (a factor of 2 in rate constant corresponds to 0.69 on the vertical axis). Agreement is also not

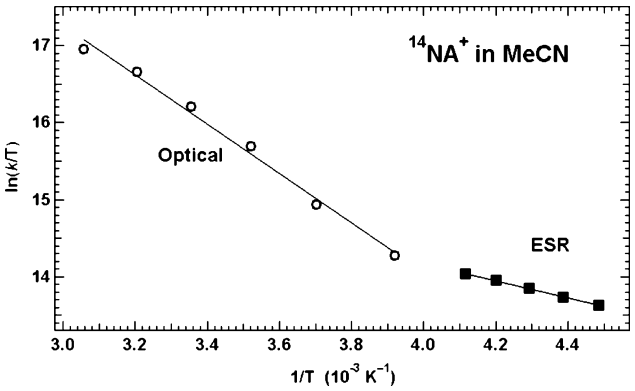

Figure 11. Comparison of optically determined k_{opt} with k_{ESR} for $\mathbf{6}^+$ ($^{14}\mathbf{NA}^+$).

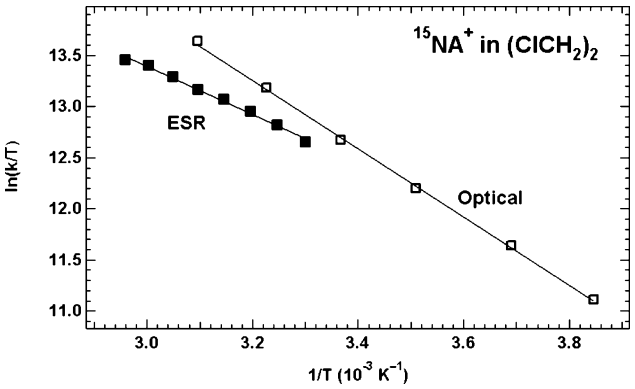

Figure 12. Comparison of optically determined k_{opt} with k_{ESR} for $\mathbf{7}^+$ ($^{15}\mathbf{NA}^+$).

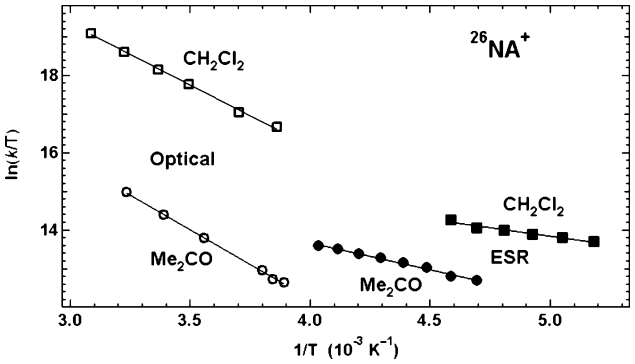

Figure 13. Comparison of optically determined k_{opt} with k_{ESR} for $\mathbf{8}^+$ ($^{26}\mathbf{NA}^+$).

(34) Nelsen, S. F.; Ismagilov, R. F.; Teki, Y. *J. Am. Chem. Soc.* **1998**, *120*, 2200−2201.
(35) Teki, Y.; Ismagilov, R. F.; Nelsen, S. F. *Mol. Cryst. Liq. Cryst. Sci. Technol., Sect. A* **1999**, *334*, 313−322.
(36) Similar calculations for all temperatures using the other solvents included in Table 4 appear in the thesis of Ageir E. Konradsson, University of Wisconsin, 2004, pp 86−127.

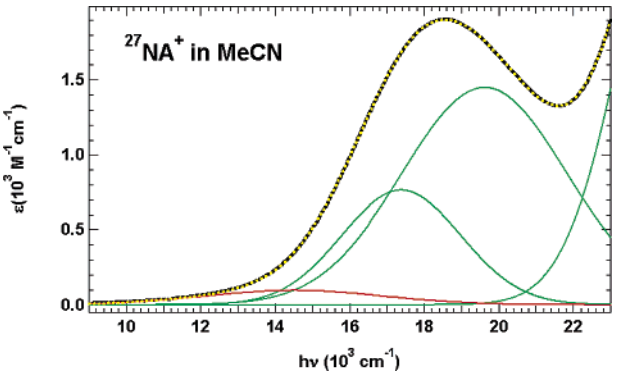

Figure 14. Multiple Gaussian fit (yellow dots) to the optical spectrum (black) for $\mathbf{9}^+$ ($^{27}\mathbf{NA}^+$) in acetonitrile. The red Gaussian is assigned as the SE band.

bad for the ^{26}**NA**-bridged compound in methylene chloride: k_{opt}/k_{ESR} is 0.93 at 259 K but drops to 0.25 at 324 K because of the difference in slopes. The k_{ESR} slopes in Eyring plots are uniformly smaller than those for k_{opt}. It is not obvious that the k_{ESR} slopes are more accurate; there are significant problems in fitting the complex ESR spectra, and although the rate constant at the temperature of maximum broadening is probably rather accurate, problems can occur as fits at increasingly higher and lower temperatures are used. The data for $^{26}\mathbf{NA}^+$ in acetone give the worst agreement between the optical and ESR rate constant for any compound we have studied. This cation is also by far the least stable of any for which we have attempted to measure the rate constant. Optical studies indicate that $^{26}\mathbf{NA}^+$ is less stable in DMSO, DMF, and acetone than in methylene chloride. We suspect, however, that the ESR rate constants, determined at lower temperature where decomposition is less of a problem, are likely to be more accurate than the optical data, which deviate in the direction expected if partial decomposition had occurred.[37] An optical rate ratio obtained for $^{26}\mathbf{NA}^+$ in methylene chloride to that in acetone of 42 (Table 7) is anomalously high; we would expect it to be closer to a ratio of 4 found by ESR (Table 1).

We were unable to detect broadening corresponding to ET by ESR for the ^{27}**NA**-bridged compound, and the optical spectrum shows why. The optical absorption in the region expected for the SE band of $\mathbf{9}^+$ is small, but we suggest that the tailing of the band at low energy is consistent with a weak band. The multiple Gaussian fit shown in Figure 14 produces a weak band of appropriate shape and position, $E_{op} = 14\,180$ cm^{-1}, $\epsilon = 110$ M^{-1} cm^{-1}, [$Q \equiv 0$ because it is a Gaussian] at 323 K in acetonitrile. Analysis of this band produces k_{opt} values of 0.03×10^8 s^{-1} in actonitrile at 323 K and 0.06×10^8 s^{-1} in methylene chloride at 322 K, which are consistent with not being able to detect any line broadening by ESR.

Discussion

The above analyses have assumed a Marcus−Hush type superexchange mechanism for the electron transfer, which leads to a surprisingly accurate prediction of the rate constants observed using the electronic coupling predicted by the optical spectrum. Robb and co-workers have discussed CASSCF calculations on electron transfer within an intervalence bis-hydrazine radical cation having $-NCH_3NH_2$ charge-bearing units attached 1,4 on a durene bridge, which led to two types of pathways that do not involve superexchange.[38] Pathways involving bridge-localized intermediates were calculated to lead to the lowest electron-transfer barriers. They occur when rotation about the NN bonds can occur, even using semiempirical calculations.[39] Such pathways are excluded by the bicyclic rings of the **Hy** charge-bearing unit, which do not allow substantial NN bond twisting, making bridge-centered cations rather high-lying excited states. The other pathway calculated involves a nonadiabatic crossing in which the NN units are almost perpendicular to the aromatic ring. This is experimentally not the case for **Hy**-centered compounds and leads to predicted barriers far higher than those observed experimentally. Our experiments support a superexchange mechanism for the electron transfer in which the positive charge is never localized on the bridge.

Conclusions

ET rates estimated for four naphthalene bridged bis-hydrazine radical cations vary significantly and show no correlation with the distance between the charge-bearing units. $^{26}\mathbf{NA}^+$ has a 100-fold larger k_{ESR} than does $^{15}\mathbf{NA}^+$ in comparable solvents, while $^{14}\mathbf{NA}^+$ has a 2.2 times larger rate constant than $^{26}\mathbf{NA}^+$ in acetone. λ clearly does not correlate with γ as it should according to dielectric continuum theory (DCT), but for the solvents studied, it does correlate with a linear combination of the Gutmann donicity number, DN, and γ. This allows the determination of λ_v, which is evaluated to be 9900 cm^{-1} for all the naphthalene-bridged radical cations. λ_s does not correlate at all with the distance between the charge-bearing units as would be expected if dielectric continuum theory worked for these compounds.

The non-Kekulé $^{27}\mathbf{NA}^+$ shows no clear superexchange transition, consistent with the small rate constant for intermolecular ET which is implied by the lack of broadening corresponding to ET by ESR, but simulations of the optical spectrum demonstrate that there is a weak band where a superexchange transition should be.

Experimental Section

Preparation of the neutral compounds appears elsewhere.[23]

Solvent Preparation: Diethyl ether was predried over KOH and used freshly distilled from sodium benzophenone ketyl. Methylene chloride and 1,2-dichloroethane were distilled from CaH_2, and acetonitrile was predried using $MgSO_4$, then distilled from P_2O_5, and finally passed over activated basic alumina prior to use.

ESR spectra were recorded using a Bruker ESP 300 E apparatus, and optical spectra that were recorded were obtained using a Perkin-Elmer PE lambda 20 double beam grating spectrometer, the concentration typically being 10^{-4} M. Sample preparation for the ESR spectra was as follows: A long-necked Pasteur pipet was closed at the narrow end with a Bunsen burner and sealed at the wide end with a septum. A solution containing the radical cation to be studied was transferred to the pipet using a syringe, the amount of which was sufficient to fill only the narrow portion of the pipet. The upper level of the solution was marked so as to be able to readjust the solvent amount. The solution was degassed using as gentle a stream of N_2 as possible for 10 min except when the solvent was methylene chloride, which then was for only 5 min to limit evaporation. Following the degassing, the solvent

(37) See Konradsson's thesis, pp 114−115, for further discussion.

(38) Ferández, E.; Blancfort, L.; Olivucci, M.; Robb, M. A. *J. Am. Chem. Soc.* **2000**, *122*, 7528−7533.

(39) Unpublished results of S. F. Nelsen.

level was readjusted by adding the appropriate degassed solvent to the pipet and mixing slightly with N_2, and the sample then used.

Preparation of Radical Cations: Variable temperature UV experiments were run as follows: Suitable $AgNO_3$ crystals were weighed out in a flame-dried test tube, equipped with a stirbar. After that, the neutral form of the compound to be studied was weighed out so that the $AgNO_3$ amounted to 0.95 equiv of the neutral form which was then placed in the same test tube as the oxidizer, and the tube then was sealed with a septum and purged with N_2. The tube was cooled to −78 °C, and MC was added slowly so as to allow it to cool before it reached the solids. The resulting solution was then stirred overnight at full speed to thoroughly break up the $AgNO_3$ crystals. The following morning, the solution was centrifuged, and the liquid was filtered through Celite into an oven dried volumetric flask. The test tube was washed three times (or until the washings were colorless if more than three washings were necessary) with MC, centrifuging, and filtering each time into the same volumetric flask. When a different solvent was desired, a solvent exchange was performed by adding some of the desired solvent and blowing N_2 through the solution, occasionally adding the second solvent until at least (usually more than) the total volume of the volumetric flask had been added. Oxidations performed in AN were run at 0 °C but also allowed to run overnight.

Optical spectra were run on a Perkin-Elmer Lambda 20 double beam grating spectrometer, samples were prepared using oven- or flame-dried glassware, and all solvents were dried and freshly distilled prior to use. The cuvettes were a matched pair of quartz cuvettes, and prior to running any samples a baseline correction (autozero) was performed using the cuvettes with the appropriate solvent in them. After the appropriate dilutions had been made (typical sample concentrations were 10^{-4} M) the spectrometer was loaded with the cuvettes, and for variable temperature spectra, the sample compartment was purged with a stream of N_2 for 0.5 h, following which the spectrometer was connected to a temperature controller and the samples were cooled to the lowest temperature used. Two spectra were run at each temperature, and the spectrometer allowed 0.5 h for temperature equilibration between temperatures.

Calculations: AM1 calculations[40] were carried out using Clark's VAMP program.[41] The (U)B3LYP calculations were carried out using Spartan'02.[42]

Acknowledgment. This work was made possible by a grant from the National Science Foundation, CHE0240197.

Supporting Information Available: Cyclic voltammetry data, intramolecular rate constants obtained by ESR (data plotted in Figure 1), ion pairing optical data for $\mathbf{7}^+NO_3^-$ and $\mathbf{8}^+NO_3^-$ in methylene chloride, simulation parameters for the optical spectra as a function of temperature of $\mathbf{6}^+$ in acetonitrile, $\mathbf{7}^+$ in dichloroethane, $\mathbf{8}^+$ in acetone and methylene chloride, and $\mathbf{9}^+$ in acetonitrile. This material is available free of charge via the Internet at http://pubs.acs.org.

JA054639K

(40) (a) AM1 calculations: Dewar, M. J. S.; Zoebisch, E. G.; Healy, E. F.; Stewart, J. J. P. *J. Am. Chem. Soc.* **1985**, *107*, 3902. (b) Holder, A. J. AM1. *Encyclopedia of Computational Chemistry*; Schleyer, P. v. R., Allinger, N. L., Clark, T., Gasteiger, J., Kollman, P. A., Schaefer, H. F., III, Schreiner, P. R., Eds.; Wiley: Chichester, 1998; p 8.
(41) Clark, T.; Alex, A.; Beck, B.; Burkhardt, F.; Chandrasekhar, J.; Gedeck, P.; Horn, A. H. C.; Hutter, M.; Martin, B.; Rauhut, G.; Sauer, W.; Schindler, T.; Steinke, T. *VAMP 9.0*; Erlangen, 2003.
(42) *Spartan'02*; Wavefunction, Inc.: Irvine, CA.